

## Subcarrier Spreading for ICI Mitigation in OFDM/OFDMA Systems

Weihua Gao, Chunjie Duan, Jinyun Zhang

TR2010-047 July 2010

### Abstract

Two of the major challenges facing OFDM/OFDMA systems are their sensitivity to frequency selective fading and ICI due to CFO or Doppler shift, especially when the subcarrier spacing becomes smaller. We propose an OFDM transceiver design that employs frequency redundant subcarrier mapping to mitigate frequency selective fading and subcarrier spreading to achieve ICI self cancellation. Both our theoretical analysis and simulation show that such a code-spread-interleaved-redundant OFDM system design offers significant (over 10dB) improvement in CIR and robust BER performance in different channel conditions.

*ICC 2010*

This work may not be copied or reproduced in whole or in part for any commercial purpose. Permission to copy in whole or in part without payment of fee is granted for nonprofit educational and research purposes provided that all such whole or partial copies include the following: a notice that such copying is by permission of Mitsubishi Electric Research Laboratories, Inc.; an acknowledgment of the authors and individual contributions to the work; and all applicable portions of the copyright notice. Copying, reproduction, or republishing for any other purpose shall require a license with payment of fee to Mitsubishi Electric Research Laboratories, Inc. All rights reserved.



# Subcarrier Spreading for ICI Mitigation in OFDM/OFDMA Systems

Weihua Gao  
EECS Department, Syracuse University  
Syracuse, NY USA  
Email: wgao03@sy.edu

Chunjie Duan and Jinyun Zhang  
Mitsubishi Electric Research Labs  
201 Broadway, Cambridge, MA USA  
Email: {duan, jzhang}@merl.com

**Abstract**—Two of the major challenges facing OFDM/OFDMA systems are their sensitivity to frequency selective fading and ICI due to CFO or Doppler shift, especially when the subcarrier spacing becomes smaller. We propose an OFDM transceiver design that employs frequency redundant subcarrier mapping to mitigate frequency selective fading and subcarrier spreading to achieve ICI self cancellation. Both our theoretical analysis and simulation show that such a code-spread-interleaved-redundant OFDM system design offers significant (over 10 dB) improvement in CIR and robust BER performance in different channel conditions.

**Index Terms**—OFDM, OFDMA, ICI, Orthogonal codes.

## I. INTRODUCTION

Orthogonal Frequency Division Multiplexing (OFDM) and Orthogonal Frequency Division Multiple Access (OFDMA) are widely adopted in current communication systems for its high spectrum efficiency and easy implementation [1], [2]. One of the recent advancements in OFDM/OFDMA system design is the increasing subcarriers density (reduce the subcarrier spacing) in order to minimize the cyclic prefix (CP) overhead.

Reduced sub-carrier spacing not only increases the transceiver complexity, more importantly, it makes an OFDM system more susceptible to frequency selective fading and inter-carrier-interference (ICI), which is caused by Carrier Frequency Offset (CFO) or Doppler effect [3].

Adding frequency diversity in an OFDM design is an effective way of mitigating the effect of frequency-selective fading. This is generally achieved by subcarrier redundancy, or channel coding. Most popular coding schemes are convolutional codes, Turbo codes and low density parity check (LDPC) codes.

To reduce ICI, we can minimize CFO by using accurate and stable local reference clocks, or implementing phase-locks (PLLs) or frequency tracking between two communicating nodes [4]. Unfortunately, neither of these solutions are viable in many systems due to the cost, power, complexity constraints, or upper layer protocols which do not support continuous transmission.

Mitigating ICI in digital domain is desirable for many reasons and there have been research work published in recent years. [5] gives a comprehensive overview of the commonly used ICI mitigation techniques. Generally all these techniques fall into three categories: i) frequency domain equalization

(FDE); ii) time domain windowing and iii) subcarrier self-cancellation. In FDE, the CFO is first estimated using training symbols and then equalized in frequency domain (after FFT) at the receiver side [6][7]. FDE minimizes ICI by compensating for CFO and thus requires an accurate CFO estimation, which is difficult to achieve when the received signal to noise ration (SNR) is low. Also the computation complexity is high in generating the correction matrix. Time domain windowing refers to techniques which use Nyquist windows other than rectangular window (e.g., Hanning window) and reduce energy leakage between subcarriers in the transmitted symbols. These windowing methods have poor performance with respect to additive channel noise [5], [8]. It also reduces the effective length of the CP and thus results in increased inter-symbol-interference (ISI). The third type is the ICI self-cancellation. Zhao et al. proposed in [9], [10] to map the same data onto an adjacent pair of subcarriers with opposite polarities and as a result, interference to other subcarriers from these subcarrier pair cancel each other.

In this paper, we propose an OFDM/OFDMA design which offers not only ICI self-cancellation but frequency diversity as well. The key features we proposed are the interleaved redundant subcarriers mapping and subcarriers spreading with orthogonal codes. We provide both theoretical analysis and numerical results on the system performance. In our simulations, the proposed designs demonstrate robust performance in both additive white Gaussian noise (AWGN) channels and dispersive channels. The spreading scheme improves Carrier-to-Interference-Ratio (CIR) by over 10 dB, and significantly lowers the bit error rate (BER).

The rest of this paper is organized as follows: Section II provides the models of OFDM systems, including mathematic relationship between CFO and ICI. It also describes in details the proposed subcarrier spreading scheme. Section III analyzes the effectiveness of the proposed ICI cancelation scheme. Section IV shows numerical results of the system performance. Section V draws the conclusions.

## II. SYSTEM MODEL

Figure 1 shows the block diagram of the proposed transmitter and receiver structure. Compared to a conventional OFDM transmitter and receiver, the key components of our design are

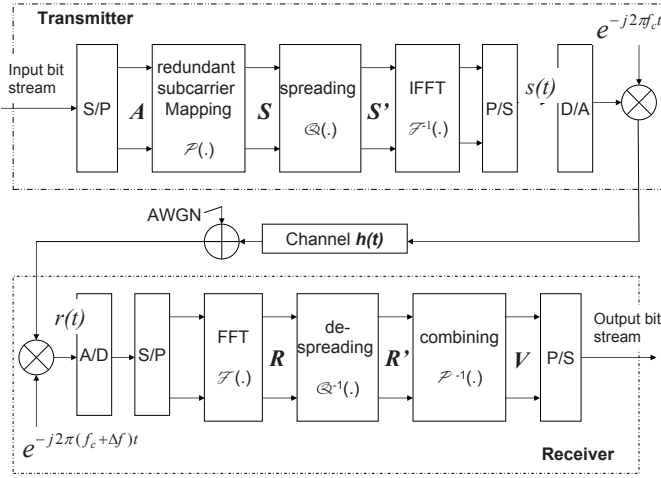


Fig. 1. Block Diagram of the Proposed OFDM System

the redundant subcarrier mapping, spreading and de-spreading blocks.

In a conventional transmitter, data to be transmitted are read in blocks. Each data block can be represented by a size- $M$  vector,  $\mathbf{A} \in \mathbb{C}^m$ ,  $\mathbf{A} = [a_1, a_2, \dots, a_m]$ , where  $a_m$  is a complex number representing a modulation alphabet based on a particular modulation scheme for the  $m$ th subcarrier (e.g., QPSK, QAM and etc.). A mapping function,  $\mathcal{P}(\cdot)$ , maps input data symbols in  $\mathbf{A}$  to a size  $N$  vector,  $\mathbf{S} = [S_1, S_2, \dots, S_N]$ .

$$\mathbf{S} = \mathcal{P}(\mathbf{A}),$$

$N$  is the number of subcarriers in an OFDM symbol.  $\mathcal{P}(\cdot)$  can be 1-to-1 mapping, which maximize spectrum efficiency, or 1-to-many. In practice, however, the mapping block also carries out pilot insertion as well as null-tone insertion in the guard band and at DC.

$\mathbf{S}$  is also referred to as the *frequency domain symbol block*. It is then transformed to a time domain sequence,  $\mathbf{s}(\mathbf{t})$ , via the inverse fast Fourier transform (IFFT) given by

$$s(t) = \mathcal{F}^{-1}(\mathbf{S}) = \sum_{k=0}^{N-1} S_k e^{j\frac{2\pi kt}{T}}, \quad (1)$$

where  $S_k$  is the frequency-domain symbol for the  $k$ th subcarrier, and  $\mathcal{F}(\cdot)$  denotes the FFT operation. Cyclic prefix (CP) is added to each output time domain sequence before it is transmitted.

The received time-domain signal,  $\mathbf{r}$ , is given by

$$r(t) = h(t) \otimes s(t) e^{-2\pi j \Delta f t} + v(t), \quad (2)$$

where  $h(t)$  is the channel impulse response,  $\otimes$  denotes linear convolution and  $v(t)$  is the additive noise. The equivalent expression in frequency domain is

$$\mathbf{R} = \mathbf{H} \cdot (\mathbf{W} \times \mathbf{S}) + \eta, \quad (3)$$

where  $\mathbf{H}$ , the channel frequency response matrix, is a diagonal matrix and its diagonal element,  $H_{k,k}$ , represents the response

of the  $k$ th subcarrier, where  $|H_{k,k}|$  is the gain and  $\angle H_{k,k}$  the phase delay.  $\eta$  is noise spectrum power,  $\mathbf{W} \in \mathbb{C}^{N \times N}$  is the ICI coefficient matrix. More details will be given in II-A.

The OFDM receiver reverses the processes occurred in the transmitter by performing the CP removal, and FFT on the received signal to produce received frequency domain symbols,  $\mathbf{R}$ , which is de-mapped to generate the received data symbol,  $\mathbf{V}$ . This processes can be expressed as

$$\begin{aligned} \mathbf{V} &= \mathcal{P}^{-1}(\mathbf{R}) = \mathcal{P}^{-1}(\mathcal{F}(\mathbf{r})) = \mathcal{P}^{-1}(\mathbf{R}) \\ &= \mathcal{P}^{-1}(\mathbf{H} \cdot (\mathbf{W} \times \mathbf{S}) + \eta), \end{aligned} \quad (4)$$

### A. Inter Carrier Interference

The severity of ICI is represented by the ICI coefficient matrix,  $\mathbf{W}$ .  $W_{m,k}$  quantifies the interference from the  $k$ th subcarrier to the  $m$ th subcarrier. In CFO free system,  $\Delta f = 0$  and  $\mathbf{W}$  is an identity matrix. (3) can be simplified to

$$R_k = H_{k,k} S_k + \eta_k. \quad (5)$$

(5) indicates that the received signal at  $k$ th subcarrier is only dependent on the transmitted signal  $S_k$ , plus the noise  $\eta_k$  and therefore is ICI free. However, the presence of CFO or Doppler effect disturbs the orthogonality between subcarriers. This is reflected in  $\mathbf{W}$ . For a given CFO,  $\Delta f$ ,  $\epsilon = \frac{\Delta f}{f_s}$  is the normalized CFO wrt the subcarrier spacing,  $f_s$ , we have [9], [11]

$$W_{k,m} = \frac{\sin[\pi(m-k+\epsilon)]}{\pi(m-k+\epsilon)} e^{-j\pi(m-k+\epsilon)}, \quad (6)$$

and the received signal on  $k$ th subcarrier becomes

$$\begin{aligned} R_k &\approx H_k \sum_{n=0}^{N-1} W_{n,k} S_n + \eta_k \\ &= H_k W_{k,k} S_k + H_k \sum_{m=0, m \neq k}^{N-1} W_{k,m} S_m + \eta_k. \end{aligned} \quad (7)$$

The first term in (7) is the received power from the signal subcarrier, the second term is the total interference from all other subcarriers. Clearly ICI is a function of  $\epsilon$ . As  $\epsilon$  grows, the power from the signal tone decreases and the interference from individual tones as well as the total interference increases as shown in Figure 2.  $W_{n,k}$  is only a function of  $(n-k)$  and therefore can be simplified as  $W_{n-k}$ , e.g.,  $W_0 \equiv W_{k,k}$ . ICI is quantified with carrier to interference ratio (CIR) to quantify ICI, defined as

$$CIR(\epsilon) = E \left[ \left| \frac{W_0}{E[\sum_{m=0, m \neq k}^{N-1} W_{k-m} a_m]} \right|^2 \right], \quad (8)$$

where  $E[\cdot]$  is the expectation over all subcarriers and input symbols. Figure 2 shows that at  $\epsilon = -0.3$ , CIR approaches 0 dB. Clearly, CFO induced ICI can be the system performance bottleneck and must be dealt with.

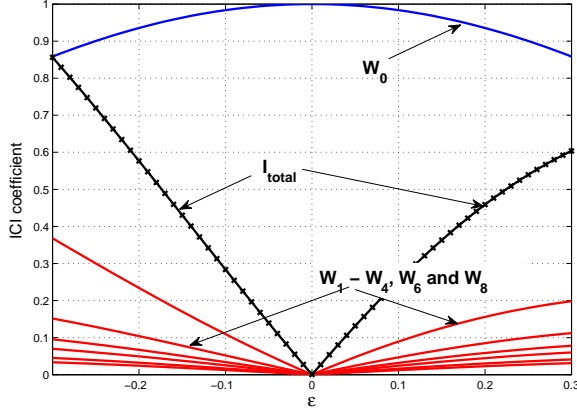


Fig. 2. ICI Coefficients vs CFO

### B. OFDM Systems with Frequency Diversity

The coherent bandwidth in most of the wireless channels is much greater than the subcarrier-spacing and therefore each subcarrier is subject to deep fading. Frequency diversity is introduced in OFDM systems to mitigate this. An easy and convenient way of providing such frequency diversity is to map each input symbol,  $a_m$ , to  $l > 1$  subcarriers, i.e.,

$$S_k = a_m, \quad \forall k \in \mathfrak{E}_m = \{k_1, k_2, \dots, k_L\}.$$

$L$  is the *degree of frequency diversity*, and  $\mathfrak{E}_m$  is the set of subcarriers assigned to  $a_m$ , referred hereafter as the *m*th *subcarrier group*. To maximize the frequency diversity, it is essential that the subcarriers assigned to the same input data are spread across the entire band. This can be achieved when an “interleaving subcarrier mapping” scheme is used. For example, assuming size- $M$  inputs vector, a diversity degree of  $L$  and omit all non-data tones, a mapping function would look as follows:

$$\mathbf{S} = \mathcal{P}(\mathbf{A}) = \underbrace{[a_1, a_2, \dots, a_m]}_{\text{1st set}}, \underbrace{[a_1, \dots, a_m]}_{\text{2nd set}}, \dots, \underbrace{[a_1 \dots a_m]}_{\text{Lth set}}, \quad (9)$$

The mapping function given in (9) maps  $M$  inputs to  $L \times M$  subcarriers. The  $m$ th input,  $a_m$  is mapped to  $L$  subcarriers,  $\{a_m, a_{M+m}, a_{2M+m} \dots, a_{(L-1)M+m}\}$ . Subcarriers in the same group have a minimum separation of  $M$  subcarriers spacing. We call this subcarrier mapping scheme “interleaved redundant subcarrier” since the subcarriers for different input symbols interleave with each others.

The corresponding receiver combines power from subcarriers that are mapped to the same input symbols. (4) is rewritten as

$$V_m = \mathcal{P}^{-1}(\mathbf{R}) = \sum_{k \in \mathfrak{E}_m} g_k R_k, \quad (10)$$

where  $g_k$  is the *combining weight* defined by the combining scheme. Two most commonly used schemes are equal gain combining (EGC) and maximum ratio combining (MRC).

EGC is simpler and in many cases sufficiently effective but MRC offers better performance in frequency selective channels [12]. The combination of redundant-mapping and combining processes effectively mitigate the frequency selective fading as it guarantees the combined SNR for a given input  $a_m$  remains acceptable when deep fading occurs on just one or a few subcarriers assigned to it.

With redundant subcarrier, CIR becomes the ratio of the *total* power of signal subcarriers for the same input symbol to the *total* power from the interfering subcarriers. Compared to an OFDM design without subcarrier redundancy, the “interleaved redundant subcarrier” mapping scheme described above offers no CIR improvement. The mathematic proof is relatively simple and will not be given here, interested reader can refer to [13], [14]. Intuitively, we can see that both the total signal power and the total interference power increase proportionally to the diversity degree  $L$ .

### C. OFDM with Spread Redundant Subcarrier

To improve the ICI performance in an OFDM system with subcarrier redundancy, we propose a *subcarrier spreading* scheme which extends the “interleaved redundant subcarrier” design discussed above but offers ICI cancelation and significant CIR improvement. The block diagram is shown in Figure 1 and details of the design are as follows:

The transmitter first maps  $M$  input alphabets,  $\mathbf{A}$ , to  $N$  subcarriers as given in (9). However, instead of taking  $\mathbf{S}$  directly as the IFFT input, a *spreading* operation is first carried out on  $S$ . The spreading operation is defined as

$$\begin{aligned} \mathbf{S}' &= \mathcal{Q}(\mathbf{S}) = \mathbf{C} \cdot \mathbf{S} \\ &= \left[ \underbrace{c_{11}a_1, c_{12}a_2 \dots, c_{M1}a_M}_{\text{1st set}}, \dots, \underbrace{c_{LM-L+1}a_1 \dots, c_{LM}a_M}_{\text{Lth set}} \right], \quad (11) \end{aligned}$$

where  $\mathbf{C}$  is a length- $LM$  *spreading sequence*. We can reformat  $\mathbf{C}$  into an  $L \times M$  matrix and each row vector in this *spreading matrix*,  $\mathbf{C}_m^R = [c_m, c_{M+m} \dots, c_{LM-L+m}]$  is the *spreading vector* corresponding to a subcarrier group. If we design  $\mathbf{C}$  such that all row vectors,  $\mathbf{C}_m^R$ , are chosen from a set of length- $L$  orthogonal codes,  $O_L$ , ICI self-cancelation can be achieved as shown in Section III.

The proposed spreading scheme does not specify the orthogonal codes that can or should be used. For example, Walsh codes based on Hadamard matrix can be used as spreading vectors. A length-4 Hadamard matrix is given as

$$\mathbb{H}_4 = \begin{bmatrix} 1 & 1 & 1 & 1 \\ 1 & 1 & -1 & -1 \\ 1 & -1 & 1 & -1 \\ 1 & -1 & -1 & 1 \end{bmatrix} \quad (12)$$

and each row vector is a length-4 Walsh code, denoted as  $\mathbb{W}_4^1$  to  $\mathbb{W}_4^4$ .

When the number of subcarrier groups,  $M$  is greater than the total number of length- $L$  orthogonal vectors available (which is generally the case), it is necessary to *reuse* the spreading

vectors, i.e., the same spreading vector is applied to multiple subcarrier groups. Two subcarrier groups are *orthogonal* ( $\mathfrak{S}_i \perp \mathfrak{S}_j$ ) if their spreading vectors are orthogonal, or *compatible* ( $\mathfrak{S}_i \parallel \mathfrak{S}_j$ ) if they share the same orthogonal code. To maximize ICI cancelation, the compatible subcarrier groups should be separated far apart.

Correspondingly in the receiver, the received symbols  $\mathbf{R}$  needs to be de-spread before combined. The output after combining is given as:

$$V_m = \mathcal{P}^{-1}(\mathbf{R}') = \sum_{k \in \mathfrak{S}_m} g_k R'_k = \sum_{k \in \mathfrak{S}_m} g_k Q^{-1}(R'_k). \quad (13)$$

$Q^{-1}(\cdot)$  denotes the de-spreading function. When Walsh codes are used as spreading vectors,  $Q^{-1}(\cdot) = Q(\cdot)$ .

Walsh codes are available for  $L = 2^k$ . All Walsh codes have only +1 and -1 as elements. This allows very simple implementation for the spreading and de-spreading operations. It is, however, not required for the coefficients to be real. By extending coefficients to complex numbers with absolute value of 1, we can find orthogonal codes for any  $L$  while preserving the transmission spectrum. For example, a set of  $L$  Fourier sequences  $\{\mathbb{F}_L^0, \mathbb{F}_L^1, \dots, \mathbb{F}_L^{L-1}\}$  form the orthonormal basis and can be used as spreading vectors. Each vector,  $\mathbb{F}_L^k$ , is defined by a Fourier series given as  $\mathbb{F}_L^k = [1, e^{\frac{2\pi k}{L}}, e^{\frac{4\pi k}{L}}, \dots, e^{\frac{2\pi k(L-1)}{L}}]$ . Cyclic orthogonal sequences can also be generated that are mutually orthogonal [15], [16]. Table I lists such a set of cyclic orthogonal codes of length-6.

TABLE I  
LENGTH-6 CYCLIC ORTHOGONAL CODE

Code Index	1	2	3	4	5	6
$\mathbb{B}_6^1$	+1	$e^{j2\pi/6}$	-1	+1	$-e^{j2\pi/6}$	-1
$\mathbb{B}_6^2$	$e^{j2\pi/6}$	-1	+1	$-e^{j2\pi/6}$	-1	-1
$\mathbb{B}_6^3$	-1	+1	$-e^{j2\pi/6}$	-1	-1	$-e^{j2\pi/6}$
$\mathbb{B}_6^4$	+1	$-e^{j2\pi/6}$	-1	-1	$-e^{j2\pi/6}$	+1
$\mathbb{B}_6^5$	$-e^{j2\pi/6}$	-1	-1	$-e^{j2\pi/6}$	+1	-1
$\mathbb{B}_6^6$	-1	-1	$-e^{j2\pi/6}$	+1	-1	$e^{j2\pi/6}$

When perfect orthogonal codes are unavailable or difficult to generate, quasi-orthogonal codes (QOC) can also be used. Due to the non-zero cross-correlation sidelobe, QOC generally offers less ICI cancelation.

### III. ANALYSIS ON EFFECTIVENESS OF ICI-CANCELATION

We now show the ICI cancelation in the proposed spread redundant carrier design. For clarity of the analysis, we ignore the pilot and null tones insertion and use the simple mapping defined in (9).

Combines (7), (11) and (13), the output of the combining

stage at the receiver can be expressed as

$$\begin{aligned} V_m &= \sum_{k \in \mathfrak{S}_m} g_k c_k R_k \\ &= \sum_{k \in \mathfrak{S}_m} g_k c_k (h_k \sum_{n=0}^{N-1} W_{n,k} c_n S_n + \eta_k) \\ &= \sum_{k \in \mathfrak{S}_m} g_k h_k W_0 c_k c_k S_k + \sum_{k \in \mathfrak{S}_m} g_k c_k h_k \sum_{n=0, n \neq k}^{N-1} W_{n,k} c_n S_n \\ &\quad + \sum_{k \in \mathfrak{S}_m} g_k c_k \eta_k \\ &= W_0 a_m \sum_{k \in \mathfrak{S}_m} g_k h_k + \sum_{k \in \mathfrak{S}_m} g_k c_k h_k \sum_{n=0, n \neq k}^{N-1} W_{n,k} c_n S_n \\ &\quad + \sum_{k \in \mathfrak{S}_m} g_k c_k \eta_k. \end{aligned} \quad (14)$$

The first term in (14) describes the power from the transmitted signal subcarrier and the second term the interfering subcarriers. The third term is from the additive noise and its total power remain unchanged with or without de-spreading, i.e.,  $E[\sum_{k \in \mathfrak{S}_m} g_k \eta_k] = E[\sum_{k \in \mathfrak{S}_m} g_k c_k \eta_k]$  given  $|c_k| \equiv 1$ .

For the clarity in the following analysis, we further assume AWGN channels ( $h_k = h$ ), and EGC ( $g_k = 1$ ) in the receiver. The first term (signal carrier) in (14) is simplified to

$$Z_m = h W_0 \sum_{k \in \mathfrak{S}_m} c_k c_k S_k = h W_0 \sum_{k \in \mathfrak{S}_m} S_k = h L W_0 a_m, \quad (15)$$

unchanged from the original non-spreading design. The interference term, however, becomes

$$\begin{aligned} I_m &= h \sum_{k \in \mathfrak{S}_m} c_k \sum_{n=0, n \neq k}^{N-1} W_{n-k} c_n S_n \\ &= h \sum_{k \in \mathfrak{S}_m} c_k \left( \sum_{n \in \mathfrak{S}_p, \mathfrak{S}_p \parallel \mathfrak{S}_m} W_{n-k} c_n a_p + \sum_{n \in \mathfrak{S}_p, \mathfrak{S}_p \perp \mathfrak{S}_m} W_{n-k} c_n a_p \right) \\ &= h \sum_{k \in \mathfrak{S}_m} c_k \sum_{n \in \mathfrak{S}_p, \mathfrak{S}_p \parallel \mathfrak{S}_m} W_{n-k} c_n a_p + h \sum_{k \in \mathfrak{S}_m} c_k \sum_{n \in \mathfrak{S}_p, \mathfrak{S}_p \perp \mathfrak{S}_m} W_{n-k} c_n a_p \end{aligned} \quad (16)$$

Rewrite the first term in (16) as

$$\begin{aligned} &h \sum_{k \in \mathfrak{S}_m} c_k \sum_{n \in \mathfrak{S}_p, \mathfrak{S}_p \parallel \mathfrak{S}_m} W_{n-k} c_n a_p \\ &= h \sum_{l=1; \mathfrak{S}_p \parallel \mathfrak{S}_m}^L c_{m+l} c_{p+l} W_{m-p} a_p + h \sum_{j \neq 0} \sum_{l=1; \mathfrak{S}_p \parallel \mathfrak{S}_m}^L c_{m+jL+l} c_{p+l} W_{jL+m-p} a_p \\ &\approx h L \sum_{p; \mathfrak{S}_p \parallel \mathfrak{S}_m} W_{m-p} a_p. \end{aligned} \quad (17)$$

The approximation is based on  $W_{m-p} \gg W_{jL+m-p}$ , i.e., interference coefficient from subcarriers far away is negligible in the overall interference. Similarly, the second term in (16) can

be approximated to

$$\begin{aligned}
& h \sum_{k \in \mathcal{E}_m} c_k \sum_{n \in \mathcal{E}_p, \mathcal{E}_p \perp \mathcal{E}_m} W_{n-k} c_n a_p \\
&= h \sum_{l=1; \mathcal{E}_p \perp \mathcal{E}_m}^L c_{m+l} c_{p+l} W_{m-p} a_p + h \sum_{j \neq 0} \sum_{l=1; \mathcal{E}_p \perp \mathcal{E}_m}^L c_{m+jL+l} c_{p+l} W_{jL+m-p} a_p \\
&= h \sum_{j \neq 0} \sum_{l=1; \mathcal{E}_p \perp \mathcal{E}_m}^L c_{m+jL+l} c_{p+l} W_{jL+m-p} a_p \\
&\ll hL \sum_{p; \mathcal{E}_p \parallel \mathcal{E}_m} W_{m-p} a_p.
\end{aligned} \tag{18}$$

Therefore we have

$$I_m \approx hL \sum_{p; \mathcal{E}_p \parallel \mathcal{E}_m} W_{m-p} a_p, \tag{19}$$

and

$$CIR_m = E \left| \frac{Z_m}{I_m} \right|^2 \approx \left| \frac{W_0}{E \left[ \sum_{p; \mathcal{E}_p \parallel \mathcal{E}_m} W_{m-p} \right]} \right|^2. \tag{20}$$

The above equation shows that at the  $m$ th symbol, the majority of interference comes from subcarriers in its compatible subcarrier groups. The larger the diversity degree, the higher the ICI. If all groups are mutually orthogonal, i.e., where each subcarrier group is assigned a unique orthogonal code, the overall CIR can be very high. Such a design would, however, be very spectrum inefficient and is hardly seen in practice.

The analysis for frequency selective fading channel, or MRC is more complicated and less insightful but can be carried out similarly. Due to the variable channel gain  $h_k$  at different subcarriers, the orthogonal groups are no longer perfectly orthogonal to the signal subcarrier group and therefore will have higher residual interference energy. As results, we can expect degraded CIR compared to AWGN channels.

Figure 3 plots the calculated CIRs based on (20) for several different spreading schemes in flat fading scenario, with the CFO,  $\epsilon$ , ranges from 0 up to 0.3. The total number of subcarriers,  $M$ , is 256. The CIR of “interleaved redundant subcarrier” with diversity degree of 4, 6 and 8 are identical and plotted as the baseline. For “spread redundant subcarrier” with diversity of 4 and 8, we use Walsh codes  $\mathbb{W}_4$  and  $\mathbb{W}_8$  respectively. For diversity of 6, we use truncated  $\mathbb{W}_8$ , i.e., all 8 codes are truncated to 6 bits.

All spreading-based design offers significant CIR improvement, with the highest CIR improvement, close to 30 dB, achieved with  $L = 8$ . Figure 3 shows that the diversity degree,  $L$ , directly affect the CIR, as it determines the spacing between compatible subcarriers. Figure 3 shows that CIR is 10 dB higher when  $L$  increases from 4 to 8. Using quasi-orthogonal codes ( $L = 6$ ) suffers little degradation.

#### IV. PERFORMANCE EVALUATION

To evaluate the effectiveness of different spreading schemes, we implement several OFDM transceivers with different redundancy and spreading schemes and simulate their BER

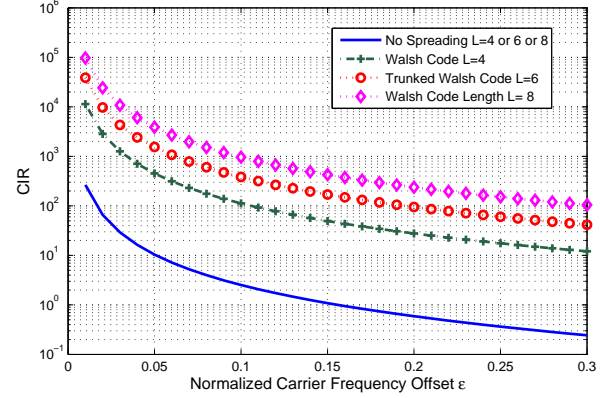


Fig. 3. Theoretical Calculation of CIR for Different Schemes

performance. The simulation is set up as follows: the center frequency of the OFDM systems is 2.4GHz and the signal bandwidth is 20MHz. Of a total of 256 subcarriers, we allocate at least 32 subcarriers as null tones in the guard band. DC tone is nulled as well. There are also 12 pilot tones evenly distributed and modulated with random generated symbols. Each tone is QPSK modulated and input symbols are randomly generated. During the simulation, we sweep  $\epsilon$  from 0 to 0.3.

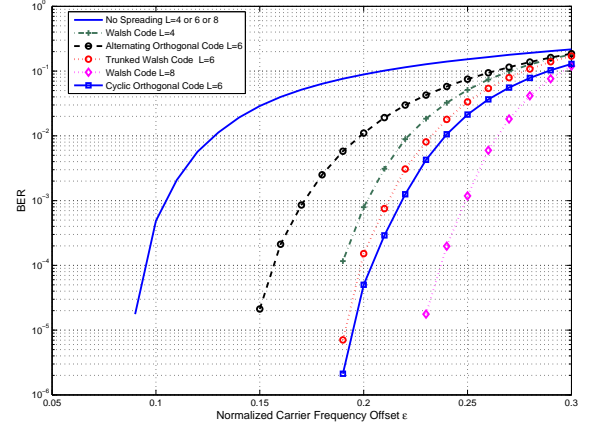


Fig. 4. BER of the OFDM system vs. CFO in flat fading channels

Our first set of simulations are carried out using flat fading channels and the results are given in Figure 4. To observe the effect of our proposed frequency spreading scheme on system BER performance, no additive noise is added to the channel. Our simulation shows that when spreading is not applied, system BER is insensitive to the diversity degree, as predicted by our analysis. Note that since the simulations use noise free channel, the frequency diversity gain after combining is not reflected in the BER.

For both  $L=4$  and  $L=8$ , Walsh codes are used as spreading vectors. For  $L=6$ , we compare three different spreading schemes: i) truncated Walsh codes, ii) alternating orthogonal codes and iii) length-6 cyclic orthogonal codes. In the first

scheme, we truncate all  $W_8$  to length-6 vectors. The truncation causes the spreading vectors to be quasi-orthogonal instead perfectly orthogonal to each other and as consequences, results in higher residual ICI. The alternating orthogonal codes scheme uses only one pair of length-6 orthogonal codes (e.g.,  $[1, 1, 1, 1, 1, 1]$  and  $[1, 1, 1, -1, -1, -1]$ ) and apply them on adjacent channels. Such arrangement results in half of the total subcarrier groups to be orthogonal to the other half of the groups, but compatible to each other within the two halves. In the third schemes,  $\mathbb{B}_6$  listed in Table I are used as spreading vectors.

The simulation shows that the second scheme has the worst BER of the three, even worse than the  $L = 4$  case. This shows that even though quasi-orthogonal suffers slight performance degradation, the CIR gain is more directly affected by the separation of the compatible groups. Even though the second scheme uses a set of 6 QOC as spreading vectors, it has much better performance than the first one. As expected, the third scheme, which uses 6 truly orthogonal spreading vectors, offers the best BER performance.

Significant spreading gain can be observed in Figure 4. For example, to achieve BER of  $10^{-3}$  and better, the maximum CFO tolerable is  $\epsilon = 0.11$  without spreading. With spreading, the tolerable CFO goes up to 0.2 for  $L = 4$  and up to 0.25 when  $L = 8$ .

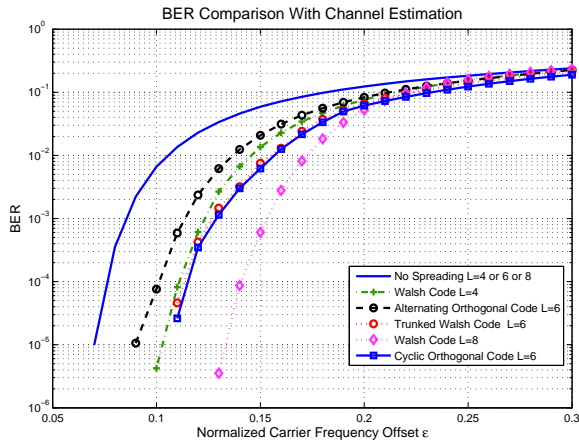


Fig. 5. BER of the OFDM system vs. CFO in indoor NLOS channels

We also compare the spreading gain in frequency selective fading channels. The channels we use are generated from indoor, non-line-of-sight IEEE 802.15.4 channel models. From the results shown in Figure 5, we can see that all scheme suffer performance loss. The spreading gain is still significant but reduced. This is attributed to the fact that the orthogonality is not maintained any more when the gain of each subcarrier is different. The gain is still directly related to the diversity degree.

Both Figure 4 and 5 show high spreading gain in the low CFO regime and it slowly reduces as  $\epsilon$  grows and in both cases, approaches 0 when  $\epsilon > 0.3$ .

In addition to OFDM systems, we simulate the performance

in OFDMA systems. A total of 256 subcarriers are assigned to multiple users. Each user has an independent clock with CFO randomly distributed within  $[-\frac{\epsilon}{2}, \frac{\epsilon}{2}]$ . Simulation results shows similar BER improvement.

## V. CONCLUSION

This paper proposed an ICI cancellation scheme for OFDM/OFDMA systems, which spreads the redundant data subcarriers with orthogonal or quasi-orthogonal codes. We present design details of both the transmitter and receiver and analysis on the spreading gain in terms of CIR improvement. Theoretical analysis and simulations are given in the paper as well. The numerical results confirm that for a given BER requirement, designs using the proposed ICI cancellation scheme are twice or more tolerant to carrier frequency offset.

## REFERENCES

- [1] 3GPP TS 36.211 V8.3.0, 3GPP Project: Technical Specification Group Radio Access Network; Evolved Universal Terrestrial Radio Access; Physical Channel and Modulation (Release 8), 2008
- [2] IEEE Std 802.16e-2005, "IEEE Standard for Local and metropolitan area networks, Part 16: Air Interface for Fixed and Mobile Broadband Wireless Access Systems," 2006.
- [3] K. Sathanathan and C. Tellambura, "Probability of error calculation of OFDM systems with frequency offset," *IEEE Transactions on Communications*, vol. 49, no. 11, pp. 1884-1888, 2001.
- [4] Z. Zhang, W. Jiang, H. Zhou, Y. Liu, and J. Gao, "High accuracy frequency offset correction with adjustable acquisition range in OFDM systems," *IEEE Trans. Wireless Commun.*, vol.4, no.1, pp. 228-237, Jan. 2005.
- [5] J. Armstrong, "Analysis of new and existing methods of reducing intercarrier interference due to carrier frequency offset in OFDM," *IEEE Trans. Commun.*, vol. 47, no. 3, pp. 365-369, Mar. 1999.
- [6] H. Moose, "A technique for orthogonal frequency division multiplexing frequency offset correction," *IEEE Trans. Commun.*, vol. 42, no. 10, pp. 2908-2914, Oct. 1994.
- [7] Z. Ye, C. Duan, P. Orlik and J. Zhang, "A Low-Complexity Synchronization Design for MB-OFDM Ultra-wideband Systems," Proc. of IEEE International Conf. on Communications (ICC'08), pp. 3807-3813, Beijing, China, May 2008.
- [8] C. Muschallik, "Improving an OFDM reception using an adaptive Nyquist windowing," *IEEE Trans. Consum. Electron.*, vol. 42, no. 3, pp. 259-269, Aug. 1996.
- [9] Y. Zhao and S. G. Haggman, "Inter-carrier interference self-cancellation scheme for OFDM mobile communication systems," *IEEE Trans. Commun.*, vol. 49, no. 7, pp. 1185-1191, Jul. 2001.
- [10] H. G. Ryu, Y. Li, and J. S. Park, "An improved ICI reduction method in OFDM communication system," *IEEE Trans. Broadcast.*, vol. 51, no. 3, pp. 395-400, Sep. 2005.
- [11] H. Steendam and M. Moeneclaey, "The effect of carrier frequency offsets on downlink and uplink MC-DS-CDMA," *IEEE Journal on Selected Areas in Communications*, vol. 19, no. 12, pp. 2528-2536, 2001.
- [12] A. F. Molisch, "Wireless Communications", Wiley, 2005.
- [13] J. Bingham, "Multicarrier modulation for data transmission: An idea whose time has come," *IEEE Commun. Mag.*, vol. 28, no. 5, pp. 514, May 1990.
- [14] T. Pollet, M. Van Bladel, and M. Moeneclaey, "BER sensitivity of OFDM systems to carrier frequency offset and Wiener phase noise," *IEEE Trans. Commun.*, vol. 43, pp. 191-193, Feb./Mar./Apr. 1995.
- [15] R. H. Barker, "Group synchronizing of binary digital systems," *Communication Theory*. London: Butterworth, 1953, pp. 273-287
- [16] S. W. Golomb and R. A. Scholtz, "Generalized Barker Sequences" *IEEE Trans. On Information Theory*. Vol 11, No. 4, Oct, 1965.